DOI 10.5162/EUROSENSORSXXXVI/PT5.241

# In-situ Synthesis of MIP Thin Films on QCM Electrodes to Sense Engineered Nanoparticles

*Mahdieh Bagheri[1,2], Illia Selvistrovich[1], Shahin Haghdoust[1], Peter Lieberzeit[1,2]*
*[1 1] University of Vienna, Faculty for Chemistry, Department of Physical Chemistry, Waehringer Strasse 42, 1090 Vienna, Austria*
*[2] University of Vienna, Doctoral School of Chemistry, Waehringer Strasse 42, 1090 Vienna, Austria*
*Peter.Lieberzeit@univie.ac.at*

**Summary:**

Herein, we report molecularly imprinted polymer (MIP) and non-imprinted polymer (NIP) thin films on quartz crystal microbalances (QCM) via in-situ polymerization to detect Engineered nanoparticles. This study focuses on controlling polymerization for controlling thickness in terms of optimal particle removal from the polymer. The sensing behavior of polymeric sensors using QCM is investigated by comparing MIP sensitivity against NIP and analyzing MIP selectivity based on particle properties.

**Keywords:** in-situ MIP, QCM measurement, Raft polymerization, Gold NPs, Magnetite NPs

## Introduction

Detecting Engineered NPs (ENPs) is particularly important due to their extensive application in biomedicine [1], environmental monitoring, and industrial processes. Established instrumental techniques, such as single particle inductively coupled plasma mass spectrometry (SP-ICP-MS), are used to detect and characterize engineered nanoparticles (ENPs) in complex environmental matrices by measuring their concentration and size distribution[2, 3]**.** To address this, recent research has focused on approaches such as molecularly imprinted polymers (MIPs). However, detecting nanoparticles requires depositing very thin films on device surfaces in a reproducible manner: they need to be thinner than the particle radius.

## Synthesizing

To achieve this, we report on synthesizing MIP and NIP thin films in situ on Quartz Crystal Microbalances (QCMs) using controlled radical polymerization, namely Reversible Addition-Fragmentation chain Transfer (RAFT). Methyl methacrylate (MMA) and EDGMA were used as the monomer and cross-linker in a molar ratio of 1:1. Herein, 4-Cyano-4-(phenylcarbonothioylthio) pentanoic acid (CPA) was chosen as the RAFT agent because of its high reactivity with acrylic monomers.

Here we mainly focused on imprinting gold NPs (GNPs) and magnetite NPs (MNPs) in the size range of 20–70 nm. For that purpose, it is essential to characterize polymer *growth in situ* as a function of polymerization time (PT) to control the thickness of polymer layers. During sensor measurements, QCMs served to assess the binding affinity of in-situ MIP films by comparing it against the corresponding non-imprinted polymers (NIPs) when detecting ENPs. To completely characterize the systems, the selectivity behavior of MIPs was studied based on different particle cores, shells, and particle sizes, respectively.

## Results

The polymer height is investigated using a network analyzer based on the change in resonance frequencies of QCM electrodes before and after polymerization for NIP. As illustrated in Fig. 1, polymer growth was measured for two series of NIP samples over 7 hours. The results indicate that maximum growth of NIP occurred between 2 to 6 PT. The polymer thickness reached the optimal height of 10 nm after 4 hours of polymerization.

Fig. 2 shows the AFM images of gold MIP surfaces after removing NPs, confirming successful imprinting of 75 nm GNPs onto the MIP surface without polymer overgrowth. The AFM height profiles of two different particle spots (1,3) display cavities in the polymer surface aligning well with the size and shape of GNPs.

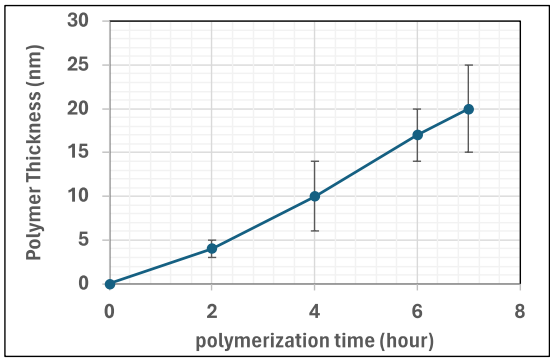


*Fig. 1. Growth of polymer thickness as a function of a polymerization time (PT=1-7 hours) for NIP*

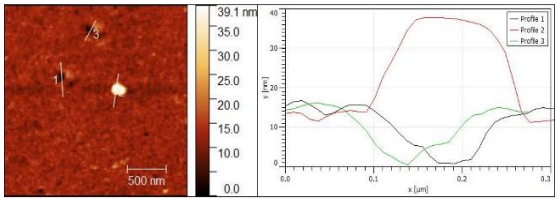


*Fig. 2. Left-hand side AFM images of GNPs MIP surface after polymerization and particle removal. On the right-hand side profile of the particle and cavity size.*

After successful imprinting, the NPs are removed from the polymer and leave behind cavities that selectively bind to the target NPs. MNPs removal was facilitated by a magnet, while for GNPs, the outer layer of NPs covered with 16-MHDA instead of PVP shell as a hydrophilic layer, ensuring effective washing off from cavities. Table 1 summarizes the responses average of MNPs MIP and the respective measured signals of NIP channels in 2mM citrate buffer as the background at c= 6e$^{15}$, 3e$^{15}$, 1.5e$^{15}$, and 7.5e$^{14}$ n/L, respectively. The corresponding limit of detection is around 8.25e$^{13}$ n/L NPs based on the noise of the bassline and slop of MIP sensor characteristics.

*Table 1. Sensor responses of both MNPs MIP and NIP sensors, at listed concentrations on QCM.*

| MNP concentration (n/L) | Average signal of two-MIP channels (Hz) | Average signal of two-NIP channels (Hz) |
|---|---|---|
| 6e $^{15}$ | -550 | -180 |
| 3e$^{15}$ | -271 | -78 |
| 1.5 e$^{15}$ | -137 | -35 |
| 7.5e$^{14}$ | -68 | -12 |

Alternatively, the surface of MIP was characterized using AFM to verify the binding of the MNPs directly into the cavities.

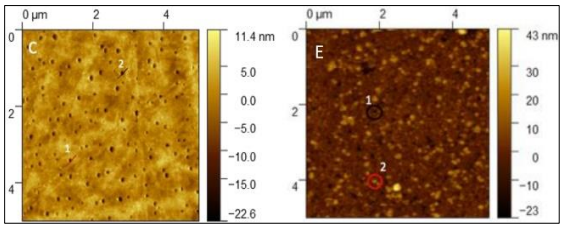


*Fig. 3. The right-hand side AFM image is the MIP surface after MNPs removal and washing the polymer surface, Left-hand side AFM image of the MIP surface after rebinding MNPs to the MIP surface.*

Selectivity studies revealed that the binding process of NPs is controlled by their shell properties, such as zeta potential, pH, and functional groups, while sensitivity strongly relies on the respective core materials. The selectivity factor of the MNPs-PVP sensor against its PVP stabilizer is approximately 9.3. Moreover, the imprinted MNPs-PVP film demonstrates high selectivity against MNPs with the same diameter but with an oleic acid shell, with a relative selectivity of only 14% compared to the MNPs-PVP sensor response. The MNP MIP sensor exhibits selectivity factors of approximately 67% and 6% against 20 nm and 60 nm SiO2 NPs with silanol surfaces, respectively. Similarly, against 20 nm and 40 nm TiO2 NPs containing surface hydroxyl groups, the corresponding selectivity factors are 48.1% and 15%, respectively. These results underscore the significant size and shell selectivity of the in-situ synthesized MIP. However, when competitor NPs and target NPs share the same size, these factors are inherently lower.

## References

1. M. Bundschuh, et al., Nanoparticles in the environment: where do we come from, where do we go to? *Environmental Sciences Europe* 30,6 (2018); doi:10.1186/s12302-018-0132-6

2. A. Grasso, M. Ferrante, et al., Chemical Characterization and Quantification of Silver Nanoparticles (Ag-NPs) and Dissolved Ag in Seafood by Single Particle ICP-MS: Assessment of Dietary Exposure, *international Journal of Environmental Research and Public Health 18, 4076 (2021);* doi:10.3390/ijerph18084076

3. Proulx, Kim et al. "Separation, detection and characterization of nanomaterials in municipal wastewaters using hydrodynamic chromatography coupled to ICPMS and single particle ICPMS." Analytical and bioanalytical chemistry 408, 5147-55 (2016); doi:10.1007/s00216-016-9451-x